Linearity Characteristics of Microwave-Power GaN HEMTs

Walter Nagy, *Member, IEEE*, Jeff Brown, *Member, IEEE*, Ricardo Borges, *Member, IEEE*, and Sameer Singhal

***Abstract*—The RF linearity of a 9-mm 10-W GaN high electron-mobility transistor (HEMT) grown on a 100-mm silicon substrate is presented. The quantitative results display promising device linearity as measured by intermodulation distortion and adjacent channel power ratio at 2.0 GHz for various power backoff levels and different quiescent points. These initial results demonstrate that larger periphery GaN HEMTs grown on silicon provide device linearity commensurate with current semiconductor device technology used for power-amplifier applications.**

***Index Terms*—GaN high electron-mobility transistor (HEMTs), linearity, RF power transistors.**

I. Introduction

As WIRELESS communication technology moves forward, the power and linearity performance requirements placed upon the power amplifiers in these systems grow more difficult to meet. Currently, silicon LDMOS power transistors are the output devices of choice for base-station power amplifiers, but as the limits of operability of these devices are reached, there will be a need for a semiconductor material that can fulfill the high-frequency and high-power requirements of the third generation of wireless technology.

Gallium nitride and its related alloys are widely acknowledged as prime candidates for high-power microwave applications due to their high breakdown field (3 MV/cm), high electron saturation velocity (2.5×10^7 cm/s), and high operating temperature. The associated AlGaN/GaN heterostructure system, enhanced by the spontaneous and piezoelectric polarization present in the heterostructure [1], [2], yields two-dimensional electron gases (2 DEGs) with high sheet charge concentration (in excess of 10^{13} cm^{-2}) and electron mobility (up to 2000 cm^2/V $\cdot$ s). The impressive electronic properties of these materials have been exploited in the form of high electron-mobility transistor (HEMT) structures to generate record-output power densities at the X- and Ku-band [3], [4].

II. GaN HEMT Structure

Historically, GaN RF power devices have been grown heteroepitaxially upon non-GaN substrate material such as SiC or sapphire with some significant advances made recently with silicon substrates [5]. All the device data presented in this paper consists of GaN HEMTs grown on 100-mm Si substrates, which are consistent with a device cross section, as shown in Fig. 1. The undoped GaN is grown on Si(111) wafers using a transition layer to accommodate the thermal expansion and lattice mismatch between the GaN and Si. Following the transition layer, a GaN buffer layer is grown and then the heterostructure field-effect transistor (HFET) structure. The HFET structure consists of an $Al_{0.23}Ga_{0.77}N$ spacer layer, an $Al_{0.23}Ga_{0.77}N$ doped region (2×10^{18} Si cm^{-3}), and an undoped $Al_{0.23}Ga_{0.77}N$ region, followed by a GaN cap.

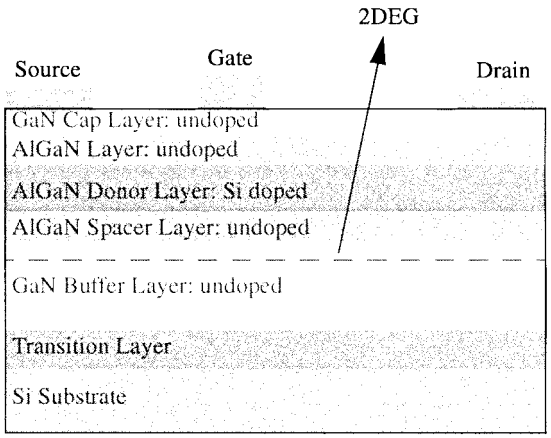

Fig. 1. Device cross section of a GaN HEMT.

The device layout investigated for this paper is a 9-mm gate periphery transistor. The device has a 1.0-μm gate length with a source–gate spacing of 1 μm and a gate–drain spacing of 3 μm. The design includes 30 fingers, each having a 300-μm gatewidth with a 25-μm pitch separating adjacent gate fingers. The multiple fingers are connected using a plated air-bridge process consisting of 3-μm-thick gold. The conservative device structure and the layout were chosen to ensure reproducibility and uniformity of device performance both across the wafer and from wafer to wafer. A photograph of the 9-mm GaN transistor layout is shown in Fig. 2.

III. DC Measurements

Pulsed current–voltage measurements were conducted on a 9-mm GaN HEMT at room temperature. Fig. 3 shows the pulsed *IV* measurements for five different gate biases and, as evident from the data, the device operates as a depletion mode transistor and pinches off near -3.0 V on the gate. The 9-mm device draws a current of 4.5 A or 500 mA/mm of periphery when the gate voltage is set to zero.

Fig. 4 depicts the transfer characteristics of the same GaN HEMT with a fixed drain voltage of 7 V. Note the peak transconductance is 166 mS/mm or 1.50 S for the 9-mm device. Both the shape and magnitude of the transconductance can be enhanced with optimization of the device structure.

Manuscript received April 15, 2002. This work was supported by the Nitronex Corporation.

The authors are with the Nitronex Corporation, Raleigh, NC 27606 USA.

Digital Object Identifier 10.1109/TMTT.2002.807684

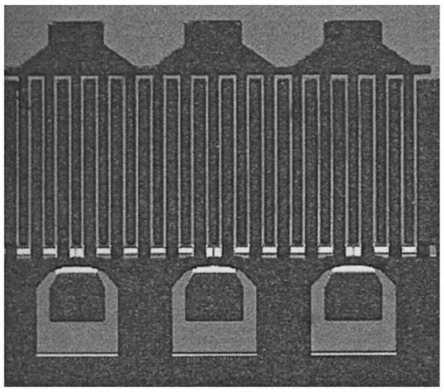

Fig. 2. Layout of the 9-mm GaN HEMT.

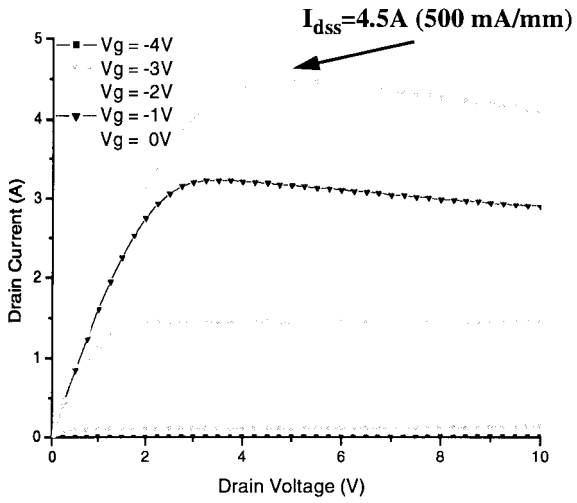

Fig. 3. Pulsed *IV* characteristics of 9-mm total periphery GaN transistor. Measurements taken with 300-μs pulsewidth and 1% duty cycle from $V_{\rm ds} = 0$.

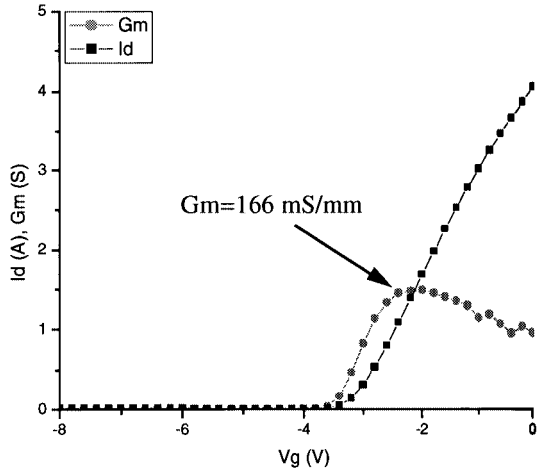

Fig. 4. Transfer characteristics of 9-mm periphery GaN transistor with constant drain voltage of 7 V.

IV. Experimental Details

The RF experimental setup depicted in Fig. 5 consists of a passive load–pull system with independent load and source mechanical tuners, external bias T's, two independent bias supplies for the gate and drain, a signal generator, and a solid-state driver

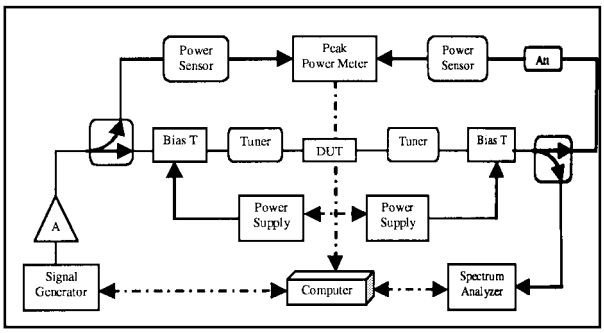

Fig. 5. Schematic of RF test measurement system.

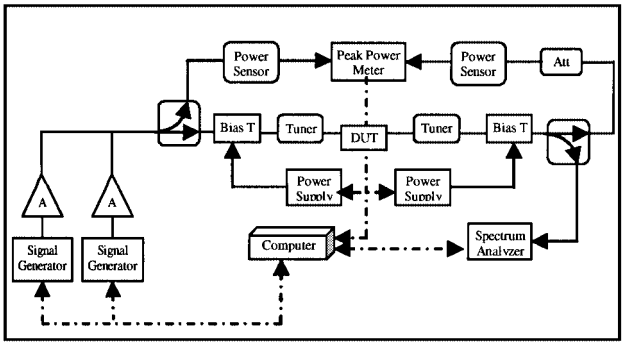

Fig. 6. Schematic of linearity test measurement system.

amplifier. The signal spectrum is monitored with a spectrum analyzer, while the RF power levels were measured by two peak power heads and a power meter. The measurement setup was under computer control during data collection.

For all RF data presented in this paper, the packaged device-under-test (DUT) had its input and output impedance's conjugate matched by the tuners to achieve maximum power gain with the input impedance matching and maximum power transfer with the output impedance matching. The DUT was mounted on a water-cooled test fixture whose base temperature was maintained at ambient during data collection.

The test setup for performing linearity measurements, as depicted in Fig. 6, is a slight modification of the previous setup, in which the latter consists of two sets of signal generators and power amplifiers for intermodulation distortion (IMD) measurements, while only one set is used for the adjacent channel power ratio (ACPR) data collection. Both the signal generator and spectrum analyzer are under computer control during linearity data collection.

An RF power sweep yields basic RF performance data and was collected with the setup depicted in Fig. 5. The RF input power was swept from 13 to 31 dBm, the output power, gain, and power-added efficiency (PAE) were collected at 2.0 GHz for the 9-mm device, as shown in Fig. 7. Under class-AB operation, the GaN HEMT yielded 10 W of RF power at the 1-dB gain compression point, which corresponds to slightly more than 1.1 W/mm, 13-dB gain, and a peak PAE of 34%. We anticipate these performance parameters will improve with further understanding of GaN device physics, the optimization of device layout, and continued process improvements in growing GaN on silicon.

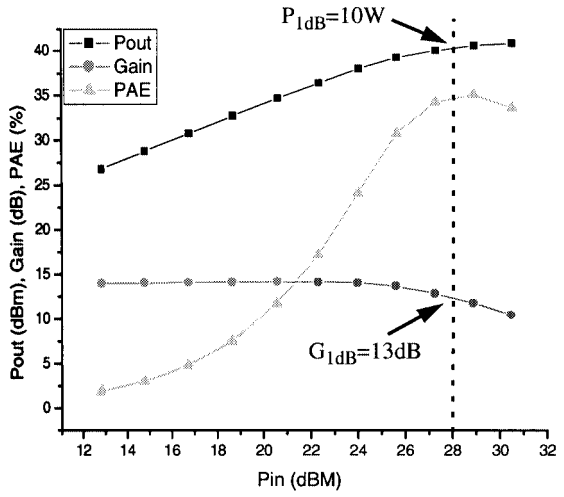

Fig. 7. RF power sweep of a 9-mm periphery GaN HEMT at 2.00 GHz and a $V_{\rm ds} = 15$ V exhibits a $P_{1\ \rm dB}$ of 10 W, a 13-dB gain, and 34% PAE. Class-AB operation.

The power density was maintained at 1.1 W/mm, which is a lower value than is typically shown for other GaN devices, in order to maintain an operating junction temperature of less than 200 °C for the larger periphery devices [6].

V. Linearity of GaN HEMTs

Wider bandwidth communication protocols such as EDGE and W-CDMA have stringent microwave signal linearity requirements, which directly impacts the linearity performance of the main base-station power amplifiers. In order to meet these demanding linearity requirements, circuit-level linearization techniques such as feedforward and digital predistortion are commonly implemented, but more linear power transistors are desirable to simplify system design [7]. For example, sufficiently linear power transistors can reduce the complexity of feedforward correction loops or eliminate them altogether in favor of less complex and lower cost digital predistortion correction.

AlGaN/GaN HEMTs comprise several key attributes toward realizing high-linearity devices. These include wide bandgaps, good transport properties, high breakdown fields, and the ability to realize heterostructures [1], [4], [5]. The first reported results on the linearity of GaN HEMTs displayed a third-order IMD product 27 dB below the carrier at $P_{1\ \rm dB}$ [4] in class-A operation at 10 GHz, for a device structure grown on an SiC substrate.

In a theoretical context, an ideally linear FET device would possess constant drain transconductance over a wide range of input gate–source voltages, i.e., the $I_{\rm d}$–$V_{\rm gs}$ relation would be perfectly linear in the region between pinchoff and forward gate turn on. In addition, the $I_{\rm d}$–$V_{\rm ds}$ relation would have vanishing knee voltage and output conductance.

As previously shown in Fig. 4, the actual $I_{\rm d}$–$V_{\rm gs}$ relation has "soft" transition regions from sub-threshold up to current saturation, leading to a transconductance profile with a diminished, or perhaps even nonexistent, constant region. Realistic device transconductance profiles make linearity analysis mathematically difficult or even intractable. Still, approximate treatments can shed some light on the major trends and contributors. Previously published Volterra-series analysis using GaAs power FETs showed that the third-order intermodulation products are roughly inversely proportional to the fourth power of the drain transconductance [8].

$$\mathrm{IMD(dBc)} = 20\log\left[\frac{3}{2g_m^2}\,P_{\rm out}\frac{|Z_{\rm out}Y_o|^2}{\mathrm{Re}(Z_{\rm out})}\,A\right].$$

Consequently, AlGaN/GaN HEMTs typically have peak drain transconductances in the 150–200-mS/mm range, a figure comparable to GaAs HFETs [7] and 3–4 times higher than Si LDMOS or SiC MESFETs [10], [11], suggesting that AlGaN/GaN HEMTs should potentially exhibit significantly better linearity than Si LDMOS or SiC MESFETs.

VI. Linearity Measurements

The linearity data was collected at a fundamental frequency of 2.00 GHz, a $V_{\rm ds}$ of 15 V, and three different bias points all in class AB.

1) IMD: For the two-tone IMD data, the first frequency tone (f_1) was set at 2.00 GHz and the second tone (f_2) was offset 100 kHz relative to the first. The third-order IMD is determined by taking the maximum output power level of the largest third-order sideband and dividing by the output power level of the smallest tone, thus creating a carrier-to-intermodulation ratio. This data is collected as the input power level is reduced such that an IMD versus power backoff curve is generated.

The maximum input power level for each of the two tones was established by determining the input power level of a single tone that results in the device's 1-dB compression point and then backing off 6 dB from this input level. The resulting two-tone output power level is the peak envelope power (PEP) [12]. To generate the IMD curve in Fig. 8, the power level of both tones were simultaneously backed off from the maximum value by equal amounts, always being within 0.2 dB of each other.

The third-order IMD was measured as a function of power back off from the 1-dB compression point for three different bias points, as shown in Fig. 8. The IMD product for all bias points can be seen to be very promising; for a 600-mA I_{dq}, the IMD linearity is -27 dBc at $P_{1\ \rm dB}$ and -48 dBc at 10-dB power backoff and is approximately equal to the 2 : 1 slope that one expects from a simple Volterra-series representation of linearity. For, a 800-mA I_{dq}, the IMD linearity at $P_{1\ \rm dB}$ also begins at approximately -27 dBc and is -51 dBc at 10-dB power backoff, which is 3 dB better than the previous case. This corresponds to a rolloff that is slightly greater than the typical 2 : 1 IMD slope.

However, for a 1100-mA I_{dq}, the IMD linearity at $P_{1\ \rm dB}$ is -25 dBc, which is worse than the previous cases, but at 10 dB power backoff is -53 dBc, which is better than the previous cases. This data implies that the linearity of a 9-mm GaN HEMT is much better than the typical 2 : 1 IMD slope from a simple Volterra-series representation of linearity.

2) ACPR: ACPR is another linearity measurement typically performed on power transistors, which employs a more sophisticated digital modulation scheme that more accurately represents modern wireless digital communication system as compared to the two-tone IMD measurement. The spectrum of a wide-band CDMA waveform is shown in Fig. 9.

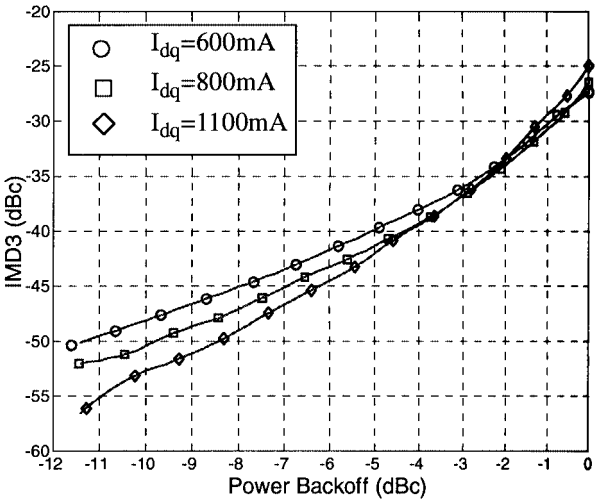

Fig. 8. Third-order IMD data versus power backoff for a 9-mm device at $I_{dq} = 1100$ mA (~25% Idss), $I_{dq} = 800$ mA (~18% Idss) and $I_{dq} = 600$ mA (~14% Idss). $f_1 = 2.00$ GHz, f_2–$f_1 = 100$ kHz, and $V_{ds} = 15$ V.

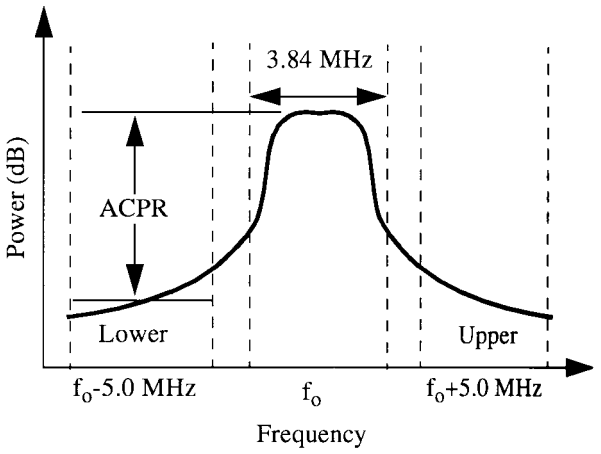

Fig. 9. ACPR for a W-CDMA waveform. ACPR is determined by taking the ratio of the larger of the two energy sidebands and dividing by the total energy in the passband.

An ACPR measurement is analogous to an IMD measurement whereby the ratio of the larger of the two integrated sideband energies is divided by the integrated passband energy. The bandwidth of integration is 3.84 MHz and the center spacing of the upper and lower bands relative to the passband is 5.0 MHz, which is the channel spacing in a W-CDMA system.

Fig. 10 depicts preliminary ACPR data from the 9-mm GaN HEMT measured in a load–pull system for three different bias points. The load–pull-based ACPR measurements utilized external bias-T's, which yield poorer ACPR results than if the same measurements were taken from a impedance-matched board with integrated biasing providing more ideal dc–RF decoupling.

At a average output power level of 2 W, which is a 7-dB backoff from the continuous wave (CW) $P_{1\,\mathrm{dB}}$ level, but less backoff from the $P_{1\,\mathrm{dB}}$ of the W-CDMA waveform, the ACPR varied between −31.5 dBc to −33.5 dBc, while at 10-dB power backoff, the ACPR varied from −33.5 dBc for a 600-mA I_{dq} to −37 dBc for the 800- and 1100-mA I_{dq}. The upper and lower ACPR bands were within 1 dB of each

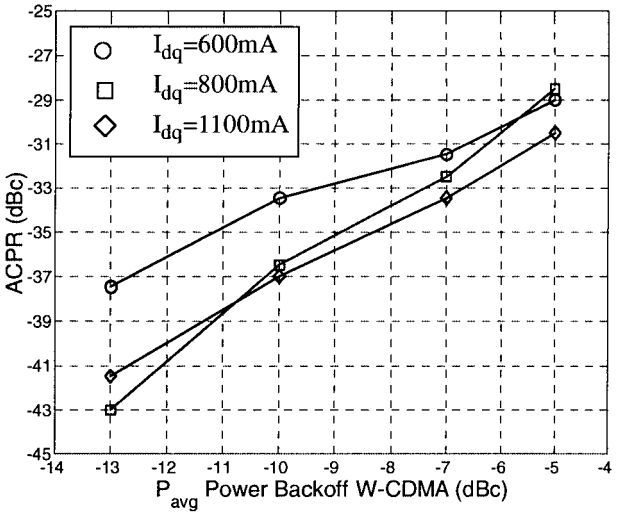

Fig. 10. W-CDMA ACPR data versus power backoff for 9-mm device at 2.00 GHz with $V_{ds} = 15$ V, $I_{dq} = 1100$ mA (~25% Idss), $I_{dq} = 800$ mA (~18% Idss), and $I_{dq} = 600$ mA (~14% Idss). The W-CDMA signal was test model 1 with 64 users and 100% clipping from an Agilent ESG-4437B signal generator as defined in 3GPP TS 25.141 V5.0.0 (2001-09) section 6.1.1.1. The waveform has a peak to average ratio (PAR) of 8.5 dB @0.1% probability and 9.8 dB @0.01%.

other for all measurements. Based upon the above data, the ACPR of the GaN HEMT appears to be less sensitive to bias current conditions, as compared to LDMOS power transistor technology. As mentioned previously, we anticipate GaN device linearity will improve with further understanding of GaN device physics, the optimization of device layout, and continued process improvements in growing GaN on silicon.

More recently, the authors have built and tested a number of larger 18-mm devices operating at a higher drain voltage of 28 V. These devices provide similar gain, efficiency, and power density as the 9-mm devices. Moreover, IMD and ACPR measurements were performed on these devices when they were mounted in an impedance-matched test board with integrated bias networks, thereby providing good dc–RF decoupling. This test setup proved to be much more favorable to ACPR measurements and resulted in ACPR data of −45 dBc at 7-dB backoff (average power of 2.0 W) from the W-CDMA compression point. The W-CDMA signal was generated on an Agilent ESG-4437B using test model 1 with 64 users and 100% clipping, the quiescent point was set at 28 V and the I_{dq} was 1.0 A.

VII. Conclusions

The structure of a 9-mm periphery GaN HEMT grown on a 100-mm Si substrate has been described. The dc, RF, and linearity characteristics as measured by IMD and ACPR at various power backoff levels and three different quiescent points at 2.0 GHz have been presented. To the best of the authors' knowledge, this is the most extensive presentation of GaN HEMT linearity data.

Acknowledgment

The authors wish to acknowledge the Nitronex Corporation, Raleigh, NC, for the growth of the GaN material, as well as

fabrication and availability of GaN HEMTs and its continued support of this study.

REFERENCES

[1] S. J. Pearton, F. Ren, A. P. Zhang, and K. P. Lee, "Fabrication and performance of GaN electronic devices," *Mater. Sci. Eng.*, vol. R30, pp. 55–212, 2000.

[2] Y. Ando, Y. Okamoto, H. Miyamoto, N. Hayama, T. Nakayama, K. Kasahara, and M. Kuzuhara, "A 110-W AlGaN/GaN heterojunction FET on thinned sapphire substrate," in *Proc. Int. Electron Device Meeting*, 2001, pp. 17.3.1–17.3.4.

[3] J. W. Palmour, S. T. Sheppard, R. P. Smith, S. T. Allen, W. L. Pribble, T. J. Smith, Z. Ring, J. J. Sumakeris, A. W. Saxler, and J. W. Milligan, "Wide bandgap semiconductor devices and MMIC's for RF power applications," in *Proc. Int. Electron Device Meeting*, 2001, pp. 17.4.1–17.4.4.

[4] T. Jenkins, L. Kehias, P. Parikh, Y.-F. Wu, P. Chavarkar, M. Moore, and U. Mishra, "Linearity of high Al-content AlGaN/GaN HEMT's," in *59th Annu. Device Research Conf. Dig.*, 2001, pp. 201–202.

[5] P. Javorka, A. Alam, N. Nastase, M. Marso, H. Hardtdegen, M. Heuken, H. Luth, and P. Kordos, "AlGaN/GaN round-HEMT's on (111) silicon substrates," *Electron. Lett.*, vol. 37, no. 22, pp. 1364–1366, Oct. 2001.

[6] S. Singhal, J. D. Brown, R. Borges, E. Piner, W. Nagy, and A. Vescan, "Gallium nitride on silicon HEMT's for wireless infrastructure applications, thermal design and performance," in *Proc. GAAS Conf.*, Milan, Italy, Sept. 23–27, 2002, pp. 37–40.

[7] P. Kenington, *High-Linearity RF Amplifier Design*. Norwood, MA: Artech House, 2000.

[8] J. Fukaya *et al.*, "A low distortion and high-efficiency E-mode GaAs power FET based on a new method to improve device linearity focused on g_m value," in *Proc. Int. Electron Devices Meeting*, 1999, pp. 405–408.

[9] S. Mass, *Nonlinear Microwave Circuits*. Norwood, MA: Artech House, 1988.

[10] C. S. Kim, J.-W. Park, and H. K. Yu, "Trenched Sinker LDMOSFET (TS-LDMOS) structure for high power amplifier application above 2 GHz," in *Proc. Int. Electron Device Meeting*, 2001, pp. 40.2.1–40.2.4.

[11] R. A. Sadler, S. T. Allen, and W. L. Pribble, "SiC MESFET hybrid amplifier with 30 W output power at 10 GHz," in *Proc. IEEE/Cornell High-Performance Devices Conf.*, Aug. 2000, pp. 173–177.

[12] K. Barkley, "Two-tone IMD measurement techniques," *RF Design Mag.*, pp. 36–52, June 2001.

Walter Nagy (M'88) received the B.S. degree from the University of Pittsburgh, Pittsburgh, PA, in 1986, and the M.S. degree from The University of Texas at Arlington, in 1989, both in electrical engineering.

In 2001, he joined the Nitronex Corporation, Raleigh, NC, where he is currently a Senior Applications Engineer. He possesses over 16 years of microwave and RF engineering experience with General Dynamics, ERIM, Lucent, and Nitronex.

Jeff Brown (M'00) was born in Lincolnton, NC, in 1972. He received the B.S. degree in nuclear engineering, and M.S. and Ph.D. degrees in physics from North Carolina State University, Raleigh, in 1996, 1998, and 2000, respectively. His graduate research concerned the development of opto-electronic devices based on the III-nitride materials system.

In 2000, he joined the Nitronex Corporation, Raleigh, NC, where he is currently a Lead Scientist, focused on the development of high-power FETs based on heterostructures in the III-nitride materials system.

Ricardo Borges (A'87–M'88) received the M.S.E.E. degree from Tufts University, Medford, MA, in 1995. He has also done graduate work in physics at the University of Massachusetts, Boston.

He is currently the Vice President of Engineering at the Nitronex Corporation, Raleigh, NC. Prior to joining the Nitronex Corporation, he was with Alpha Industries, M/A-COM, Cree, and Avant!, where he was an Engineer and Manager in process development, device design, and simulation of various semiconductor technologies, including GaAs MESFET, Si bipolar, Si LDMOS, and SiGe HBTs.

Sameer Singhal received the B.S. degree from the Georgia Institute of Technology, Atlanta, in 1999, and the M.S. degree from Stanford University, Stanford, CA, in 2001, both in materials science and engineering.

He is currently with the Nitronex Corporation, Raleigh, NC. He possesses two years of prior simulation experience with the Computational Fluid Dynamics Research Corporation (CFDRC).